


# Reed Switch Overcurrent Protection: New Approach to Design

Dauren Dzhambulovich Issabekov <sup>1,\*</sup> , Zhassulan Bakutzhonovich Mussayev <sup>1</sup>, Vadim Pavlovich Markovskiy <sup>1</sup>, Aleksandr Petrovich Kislov <sup>2</sup> and Dariya Sansyrbayevna Urazalimova <sup>2</sup>

<sup>1</sup> Department of Electrical Power Engineering, Faculty of Energetics, Toraighyrov University, Lomov Str. 64, 140008 Pavlodar, Kazakhstan; zhaslan200890@gmail.com (Z.B.M.); vadim.markovski1967@gmail.com (V.P.M.)

<sup>2</sup> Department of Electrical Engineering and Automation, Faculty of Energetics, Toraighyrov University, Lomov Str. 64, 140008 Pavlodar, Kazakhstan; kislovap2020@gmail.com (A.P.K.); ud1584878@gmail.com (D.S.U.)

\* Correspondence: daurenissabek1715@gmail.com

**Abstract:** The problem of getting rid of expensive and metal-intensive current transformers has been declared by CIGRE as strategically important for the electric power industry. However, almost all traditional current protections receive information from measuring current transformers. In this work, a resource-saving reed switch overcurrent protection without current transformers is suggested, which can be used as an alternative to traditional current protections for 6–10 kV electrical installations connected to a switchgear cell. The protection is designed following the novel method we have developed based on inductance coils. Inductance coils measure the electromotive force under different operation modes of an electrical installation and at different points inside the switchgear cell it is connected to; the EMF values are recalculated in the values of magnetic induction, and reed switches are mounted instead of inductance coils at the points where the magnetic induction is maximal. Moreover, these values are sufficient to detect phase-to-phase short circuits in the electrical installation. The dependence of the induction value on the position of an inductance coil inside the cell is derived with the use of the simplest formula of the Biot–Savart law. The results can be used at large and small industrial enterprises, electric power stations, and substations of plants; they can be interesting for the scientific community because they help to solve the topical problem of the electric power industry.

**Keywords:** current; induction; inductance coil; reed switch; cell; overcurrent protection; current transformer



**Citation:** Issabekov, D.D.; Mussayev, Z.B.; Markovskiy, V.P.; Kislov, A.P.; Urazalimova, D.S. Reed Switch Overcurrent Protection: New Approach to Design. *Energies* **2024**, *17*, 2481. <https://doi.org/10.3390/en17112481>

Academic Editors: Pinjia Zhang, Xiaoyan Huang, Cungang Hu and Wen-Ping Cao

Received: 22 March 2024

Revised: 29 April 2024

Accepted: 14 May 2024

Published: 22 May 2024



**Copyright:** © 2024 by the authors. Licensee MDPI, Basel, Switzerland. This article is an open access article distributed under the terms and conditions of the Creative Commons Attribution (CC BY) license (<https://creativecommons.org/licenses/by/4.0/>).

## 1. Introduction

The International Council on Large Electric Systems CIGRE has declared the problem of abandoning the use of expensive and metal-intensive current transformers as strategically important for the electric power industry. Almost all traditional current protections receive information from measuring current transformers. Therefore, it is necessary to find an alternative to heavy, big, and expensive measuring current transformers and protections based on them. Works on the creation of alternative resource-saving relay short-circuit protection devices without metal-intensive current transformers with metal cores for various electrical installations have been started in the second half of the past century and remain topical today [1–3].

Nowadays, microprocessor relay protection devices are commonly used. However, they are tens and hundreds of times more expensive than electromechanical or semiconductor protection devices, and their reliability is not higher because of vulnerability to cyberattacks via the Internet [1,4]. To increase the reliability, it is necessary to find an alternative to measuring current transformers and current protections, from which they receive information [5]. One of the promising ways to design the relay protection devices without measuring current transformers is the use of reed switches, which have a number of advantages in comparison with other magnetosensitive elements [6–24].

In works [6,7,13,14,16,17,24], current protections based on reed switches are considered. A magnetically controlled contact as part of an electrical circuit is a contact that changes the circuit state through mechanical closure or opening when exposed to a magnetic field. This contact placed in a sealed glass cylinder is called a reed switch and is used as an elemental base in relays, buttons, switches, and other electrical devices. In the experiments conducted in this work, a reed switch, being an element of an electric circuit, acted as a measuring element. Under the influence of an external magnetic field produced by a conductive bus or a permanent magnet, the ends of reed switch contacts are magnetized and take up, thus completing the electrical circuit. The most important advantages of reed switches as an elemental base for current protections are the capability of simultaneously functioning as a fast-acting current relay and current transformer; the transmission of a control signal through control circuits instead of measuring circuits; and a long service life.

However, reed switches have some disadvantages common for all other magnetically sensitive elements in protection devices: sensitivity to external magnetic fields from both neighboring phases next to the one it is fixed under and current-carrying phases of neighboring electrical installations. In addition, sticking of reed switch contacts is possible, although very rare. These disadvantages can be easily overcome in practice through adjusting against external magnetic fields by increasing the number of reed switch contact actuations without reducing its characteristic speed and applying test and functional diagnostics of faults of the whole protection device. The fundamental reason for using reed switches in relay protections is saving resources in current protections based on them compared to protections based on current transformers with metal cores.

Magnetodiodes and magnetotransistors are discussed in [8]. The magnetodiode effect arises when placing a semiconductor with non-equilibrium conductivity in a magnetic field, which is manifested through the injection of carriers from a p-n junction when a direct current passes through diodes. The disadvantage of magnetodiodes in measuring currents is their inherent nonlinearity, which limits the scope of their use.

Magnetotransistors have stable temperature, linearity, and a wide frequency range. They convert current into voltage and are designed for measuring alternating current, direct current, and pulsating current in a wide range and providing information about the current in the form of a digital or analog output signal; the galvanic isolation of circuits involves the transmission of a signal about the current to devices and protection elements. The output parameter of a magnetotransistor is proportional to instantaneous magnetic field induction. Due to the absence of windings and a magnetic core, it is much smaller and lighter than conventional current transformers with metal cores. Magnetotransistors do not need significant output power, which is their advantage over current transformers. Their disadvantages are the following: they need a current source, have noise, include a significant number of sensors, and react to a magnetic field modulus, and their parameters change with the ambient temperature.

In works [9,10], the use of magnetoresistors is considered. Magnetoresistors are characterized by the dependence of resistance on magnetic induction  $R = f(B)$ . They respond to a magnetic field modulus; that is why they have not been widely used for current measurement.

Work [10] studies Hall sensors. When a magnetic field acts on a current that flows through a semiconductor, the Hall effect arises. The main properties of a Hall sensor are its capability of inducing an electromotive force when being placed in a magnetic field and a current is flowing through it and the emergence of a useful voltage in the direction transverse to a signal. Protection relays on the basis of Hall sensors use the comparison between two electrical parameters, for example  $E_1$  and  $E_2$ , which should be functions of relay voltage  $U_p$  and current  $I_p$  or one of these two characteristics. Drawbacks of Hall sensors include complexity of measuring circuits, residual voltage, need for a stable supply of their circuits, susceptibility of currents of neighboring phases of an electrical installation, deviation between parameters of sensors from the same batch, and need for compensating for temperature effects.

Works [11,12] consider current protections with current sensors based on Rogowski coils. A Rogowski coil is a wire wound on a non-magnetic core placed around the conductor where the current is to be measured. Unlike a traditional current transformer, a Rogowski coil does not contain a metal core and, therefore, does not saturate. A signal from a Rogowski coil has minimal voltage. Weight and size of a coil are much lower than those of current transformers; the range of current is quite wide; it is not subject to saturation. Their disadvantage is low measurement accuracy.

Work [15] studies the optimal use of fault current limiters for coordinating operation of directional overcurrent relays without the need to reset these relays regardless of the layout of distributed generation. It is necessary to maintain the coordination of overcurrent relays and minimize the cost of fault current limiters. Hence, the problem of arranging and sizing these limiters is formulated as a multicriteria optimization problem with constraints. Multicriteria optimization is used to determine the optimal positions and size of short-circuit current limiters. The suggested algorithm is applied to mesh and radial power systems with different layouts of distributed generation. The problem of the coordination of overcurrent relays is studied for the case where both directional and non-directional overcurrent relays are present in a system.

In [18], the improvement in performance of distance relays is considered. In the stressed state of a power system, the power in transmission lines can decrease and affect the apparent impedance of a distance relay, thus causing its malfunction. This situation can lead to a cascading outage and, hence, a power outage. Proper coordinated interlocking and tripping circuits for distance relays become important to avoid the failure of such a relay and maintain the integrity of the system. A fault-tolerant protection circuit is suggested, which uses adaptive adjustment, thus preventing relay failures under the stressed state of a system. The circuit receives pre-alarm data from two finite-distance relays to perform the suggested adaptive relay adjustment.

In [19], measurements of electric current with an improved current transformer are considered. The two main problems in protective current transformers are saturation and residual flux in their ferromagnetic cores. To minimize the effects of high saturation and residual flux, a current transformer with a gap core can be used. Although this solves both problems, studies show that gaps in a ferromagnetic core can cause mechanical brittleness compared to a closed core.

Work [20] describes monitoring of electric current based on a magnetoresistive sensor. Such monitoring can facilitate preventive actions in an electrical distribution network to reduce power overloads, improve transmission efficiency, and ensure network reliability. Non-invasive current sensing devices are promising because they do not require contact with dangerous high voltages and their installation is much simpler compared to invasive current sensing devices. However, existing non-invasive current measurement devices, such as current clamps and Rogowski coils, are only applicable to single-core underground power cables. A non-invasive technique for monitoring currents in a multicore underground power cable through measuring a generated magnetic field around the cable surface was developed in that work. Additional magnetic fields generated by induced currents and leakage currents in cables were first estimated. Magnetoresistive sensors in the form of a circular array were used to measure a magnetic field around the cable surface, and a three-layer shielding was developed to reduce the effects of external interference.

In [21], electric current was measured with a magnetic sensor. Innovative methods for a wide-range measurement of electric current remain an urgent research problem in modern power systems. Conventional methods based on magnetic field readouts enable non-contact current sensing by interpreting magnetic flux density into electric current, such as the Hall effect and Rogowski coil arrangement. A magnetic sensor has been widely used for current measurement due to its small size, low cost, high response frequency, and high sensitivity. However, the measured magnetic field is strongly affected by a superposed unwanted magnetic field. In that work, a four-sensor array design was suggested to solve this problem.

Work [22] considers electric current measurement by current transformers with the use of a new technique for their calibration. Measurements in power systems are often made using current and voltage signals received from the secondary circuits of measuring transformers. Errors introduced by these transformers are commonly considered as a component of input errors in supervisory control, data acquisition, and vector measurements. Correcting these errors by calibration is an expensive option; it is used in a few special cases. This work suggests a new method for calibrating measuring transformers with the use of vector measurements by estimating the correction factors of the transform ratio of the transformers and the phase angle. This method focuses on the main frequency component of vector measurements. Unlike some methods described in the literature, it does not require precise models of measuring transformers and can be performed as often as necessary to update the calibration.

In [23], the use of an optical current sensor for measurement and protection in high-power systems is discussed. Power transformers are commonly used in the electric power industry. However, under high voltage, they can be magnetically saturated or damaged due to heat, short circuits, and atmospheric electrical discharges. Therefore, protection and reliable insulation systems are required, which demand expensive technical maintenance procedures. In the face of these challenges, optical current sensors have many advantages and can be an alternative to conventional technologies. Optical sensors are less demanding in terms of isolation, which provides immunity to electromagnetic interference. Depending on the configuration and transformation mechanism, they ensure a higher dynamic range, wider operating bandwidth, and no hysteresis loop.

Principles of constructing overcurrent protections, for example, of transmission lines; differential protections of lines; and so on have already been developed. However, these principles cannot always be used without additional research due to the variety of arrangement of busbars inside switchgear cells and electrical installations [25–28]. When designing an overcurrent protection system for electrical installations connected to a working switchgear cell, in addition to the development of structures for mounting reed switches, there is a need to take into account the interference both from the currents within the working cell the reed switches are mounted in and from the current-carrying busbars of a neighboring cell.

The aim of our work was to develop a method for constructing overcurrent protections for 6–10 kV electrical installations connected to switchgear cells and to design an overcurrent protection device that can serve as an alternative to traditional current protections with measuring current transformers and current relays with metal cores and enables resource saving.

## 2. Materials and Methods

To construct the overcurrent protection, it is necessary to study the magnetic field inside a working cell. For that, we used inductance coils mounted inside the cell. Alternating current of 0 to 600 A is supplied to the current-carrying busbars of the working and neighboring cells. When the current is applied at the output of an inductance coil, an electromotive force of 0.024 V to 0.2 V is induced. The inductance coils' response to the sum of magnetic currents should be noted: from the current-carrying busbar opposite to which they are fixed inside the working cell, from current-carrying busbars of neighboring phases of the working cell, and from the neighboring cell. The points where the electromotive force is maximal are determined. Reed switches are mounted at these points instead of inductive coils.

## 3. Experimental Section

To determine the magnetic fields inside switchgear cells, we performed an experiment where the above procedure was implemented. The experiment was carried out with KRU-2 working cell (1) 90 cm wide and K-63 neighboring cell (2) 70 cm wide [29,30]. The cells were placed in a room. First supporting wall (3) was on their left and second supporting

wall (4) was at the rear (Figure 1). The equipment included in the experimental setup is presented in Table 1.

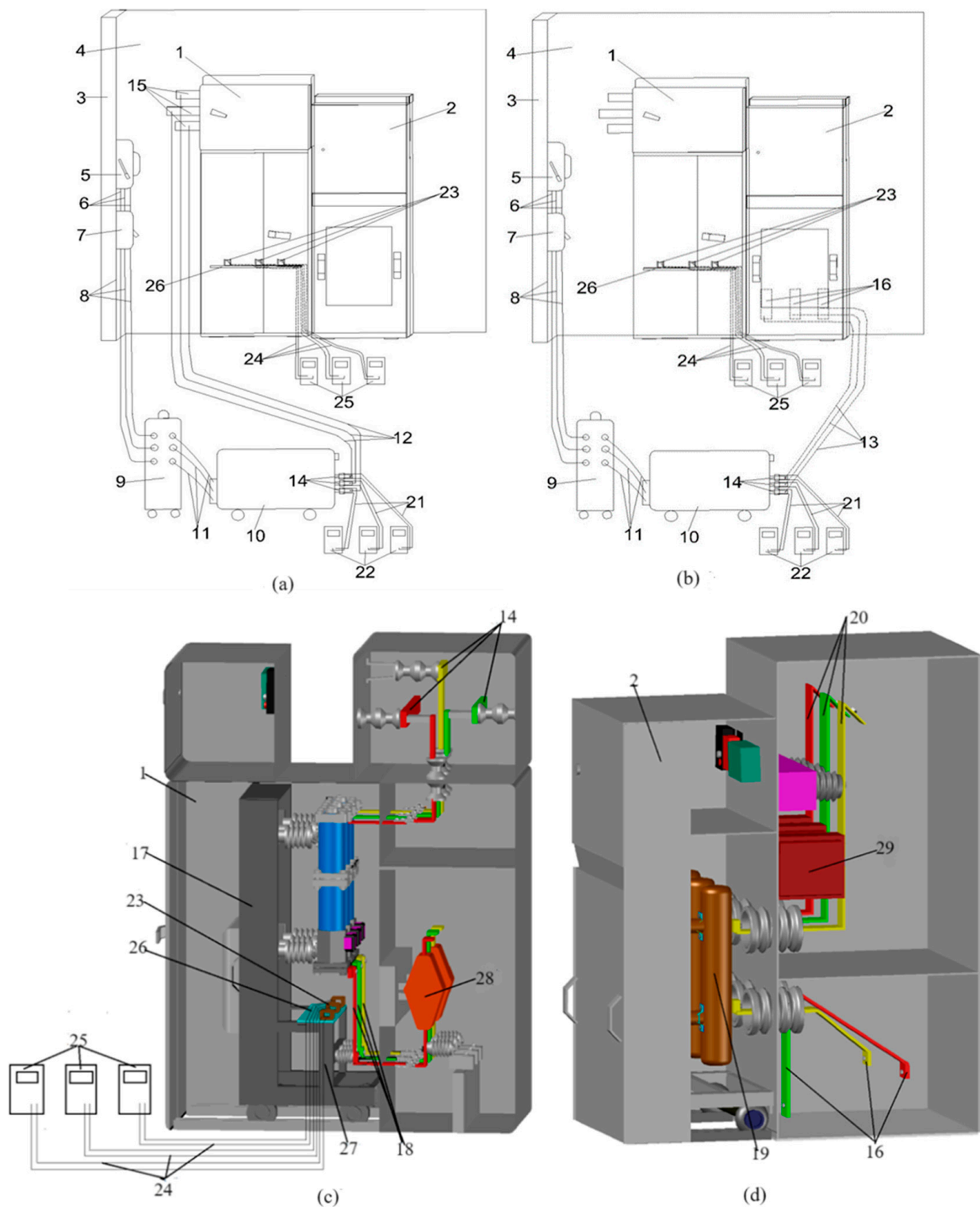


**Figure 1.** Experimental setup: (a) working cell; (b) neighboring cell; sections of (c) working and (d) neighboring cells, with determination of magnetic field values in working cell.



**Table 1.** Experimental setup composition.

No.	Component	Quantity
1	Working (1) and neighboring cells (2)	2
2	Three-phase load transformer (10)	1
3	Power cables (12 and 13)	2
4	Current transformers (14)	1
5	Second current-carrying busbars (18)	1
6	Wires (21 and 24)	2
7	Inductance coils (23)	1
8	Current (22) and electromotive force recorders (25)	2
9	Plate (26)	1

Two options of supplying alternating current to the current-carrying busbars of two cells were considered (Figure 1a,b). The experimental setup included three-phase switch (5) for alternating current voltage  $U_H = 380$  V and rated current  $I_H = 100$  A, with type VA57-35 circuit breaker (7) with rated current  $I_H = 100$  A. Cable (6) is connected to circuit breaker (7). Three-phase voltage stabilizer (9) is connected to cable (8). The primary winding of three-phase load transformer (10) is connected by cable (11) to three-phase voltage stabilizer (9). The secondary winding of the load transformer is connected by power cable (12) (Figure 1a) and (13) (Figure 1b) through the windows of first current transformers (14) to first current-carrying busbars (15) and (16) of cells 1 and 2. The current flows from the first current-carrying busbars of working cell 1 through the closed contacts of breaker (17) to second current-carrying busbars (18). The axes of busbars 18 are centered at 68 cm (phase A), 45 cm (phase B), and 22 cm (phase C) from the right wall of cell 1. In neighboring cell 2, the current flows from first current-carrying busbars (16) through the closed contacts of breaker (19) to second current-carrying busbars (20).

Three-phase load transformer 10 is mounted opposite the front side of cell 1. Power cables 12 and 13 were laid on the left side of working cell 1 and on the right side of neighboring cell 2. Such routing of power cables 12 and 13 enables detecting magnetic fields inside cell 1. Current recorders (22) are connected to the secondary windings of current transformers 14 using wires (21). The magnetic field sensors were three tested inductance coils (ICs) (23) from an MKU-48 intermediate relay without a metal core; they were connected by cables (24) to electromotive force recorders (25) [31]. In the experiments, the ICs were used only to determine the electromotive force values at one or another point of working cell 1. Fluke 87V multimeters were used as the current and electromotive force recorders. Inductance coils 23 inside cell 1 were mounted on plate (26) made of dielectric material (textolite),  $90 \times 18 \times 0.5$  cm in size, with a scale with 1 cm division. The distance between the plane of the location of second current-carrying busbars 18 and the points of mounting ICs 23 on plate (26) was 12, 18, and 24 cm respectively. Magnetic induction was measured at 21 points on plate (26).

Preparation for the experiments: Plate (26) with ICs 23 was mounted horizontally on frame (27) of the breaker (17) truck inside working cell 1. Plate 26 was fixed at three altitudes above frame 27: 0 cm (on frame 27), and 6 and 12 cm. The measured distance and, hence, the IC mounting points on plate (26) are counted from the right to the left wall of cell 1. Inputs L1 of the primary winding of second TPL-10-150 and TLO-10-300 current transformers (28 and 29) were connected to second busbars (18 and 20) of cells 1 and 2. Outputs L2 of this winding were short-circuited in the form of corresponding short circuits [5]. The secondary winding of current transformers (28 and 29) was also short-circuited during the experiments. Three-phase voltage regulator 9, load transformer 10, and the bodies of cells 1 and 2 were grounded according to the safety rules [32]. To determine the electromagnetic field strength inside working cell 1, three-phase switch 5 is closed (Figure 1a,b) and alternating current from three-phase load transformer 10 is supplied by three-phase voltage regulator 9 through circuit breaker 7 to first current-carrying busbars 15 of cell 1 in the first option and to first current-carrying busbars 16 of cell 2 in the second

version through power cables 12 and 13. The strength of the current flowing through busbars 15 and 16 is controlled by readings of current recorders 22.

The experiment with current flow through three, two, and one current-carrying busbars of the working and neighboring cells simulated three-, two-, and one-phase short circuits. The initial value of the current flowing through the first (15 and 16) and the second (18 and 20) current-carrying busbars of cells 1 and 2 was  $I = 100$  A. Electromotive force (EMF) from ICs 23 mounted on plate 26 inside cell 1 was measured and recorded by EMF recorders 25. The current was passed by turns, first through current-carrying busbars of the working cell (Figure 1a), and then through busbars 16 of the neighboring cell (Figure 1b). The ends of the primary windings of second current transformers 28 and 29 were short-circuited in the form of three-phase and two-phase short circuits.

Inductance coils 23 are moved from the initial point 0 cm to the final point 90 cm in cell 1 and the electromotive force is permanently recorded. Increasing the current by 100 A up to 600 A at each measurement point, the procedure of measuring the electromotive force is repeated. When current flows through first busbars 15 of cell 1, the electromotive force is measured and recorded at the points located at a distance of 12 cm from the plane of second busbars 18 and then at points spaced 18 and 24 cm apart from this plane (second and third row) at the first, second, and third positions of plate 26 inside cell 1.

When simulating a single-phase short circuit, the current first flows through one first current-carrying busbar 15 of cell 1 followed by the alternation of other phases, and then through first current-carrying busbars 16 of neighboring cell 2 in the same way. Power cable 12 and 13 coming from load transformer 10 were connected to one of first current-carrying busbars 15 and 16 of cells 1 and 2 at one end. Another power cable 12, and 13, was connected to the output of primary windings L2 of second current transformers 28 and 29 of cells 1 and 2 at the first end, and its second end was connected to load transformer 10. The electromotive force from the external profile sides of cell 1 is measured with one IC 23 attached thereto with double-sided adhesive tape.

Within the experiments, the sensitivity of the current protection mounted in operating cell 1 to external short circuits, i.e., to faults in the electrical installation connected to neighboring cell 2, was also studied. For this purpose, the values of induction inside cell 1 during normal operation (three-phase) of the electrical installation connected to it are compared with its values during three-, two-, and single-phase short circuits in the electrical installation connected to cell 2.

#### 4. Results

Figure 1b shows the scheme of the connection of power cables 13 to first current-carrying busbars 16 of cell 2 with simulation for cell 1 of an external (three-, two-, and single-phase) short circuit from the electrical installation connected to cell 2. The magnetic induction is measured with the same ICs 23 at the same points under the same values of the current and at the same distances from the plane of second busbars 18 inside cell 1 (see the previous section). Based on the measured values of electromotive force, the magnetic field induction is calculated by the formula

$$B_{\text{exp}} = \frac{E_{\text{exp}}}{2\pi\omega S f} \mu\text{T} \quad (1)$$

where  $E_{\text{exp}}$  is the electromotive force from IC 23 terminals during the experiments;  $\omega$  and  $S$  are the number of turns and cross-sectional area of the IC; and  $f$  is the industrial frequency.

For example, for the current  $I = 100$  A passing through busbars 11 at point 0 cm,

$$B_{\text{exp}0} = \frac{E}{2\pi f S \omega} = \frac{24 \times 10^{-3}}{2 \times 3.14 \times 50 \times 767 \times 10^{-6} \times 8000} = 12 \times 10^{-6} \text{ T}$$

The points for mounting reed switch protections inside cell 1 are determined from the maxima of the calculated induction; that is, reed switches are mounted instead of ICs 23.

The dependence of magnetic induction on the current and the points of fixing ICs 23 on plate 26 relative to second current-carrying busbars 18 is shown in Figure 2 for the cases of three-, two-, and single-phase short circuits when plate 26 is at the first position and the distance from busbars 18  $h = 12$  cm.

A possibility of a two-phase short circuit occurring in the electrical installation connected to cell 2 during the nominal operation of the electrical installation connected to cell 1 is considered through the accounting coefficient  $K_{acc}$ . This coefficient simultaneously takes into account the resultant induction inside cell 1 during the normal operation of its electrical installation and the resultant induction during a short circuit in the electrical installation of cell 2. The resultant induction also takes into account the so-called phase effect, i.e., the inductions caused by the distortion of the magnetic field from different metal structures, including inside the bodies of cells 1 and 2, when current is flowing through one and neighboring busbars.

The accounting coefficient is defined as

$$K_{acc} = \frac{B_{\text{nominal working cell}} \times 10^{-6}}{B_{\text{short-circuit of a neighboring cell}} \times 10^{-6}} \quad (2)$$

Figure 3 shows the magnetic induction versus the current and the points of mounting ICs 23 on plate 26 inside cell 1 and at a distance  $h = 12$  cm from second current-carrying busbars 18 when the current flows through three (ABC), two (AC), and one (A) current-carrying busbars of cell 2.

Tables 2 and 3 show the values of the coefficient  $K_{acc}$  at the nominal operation (three-phase) mode of the electrical installation of cell 1 and two-phase short circuit between phases A and C, as well as the single-phase short circuit in phase A in the electrical installation of cell 2.

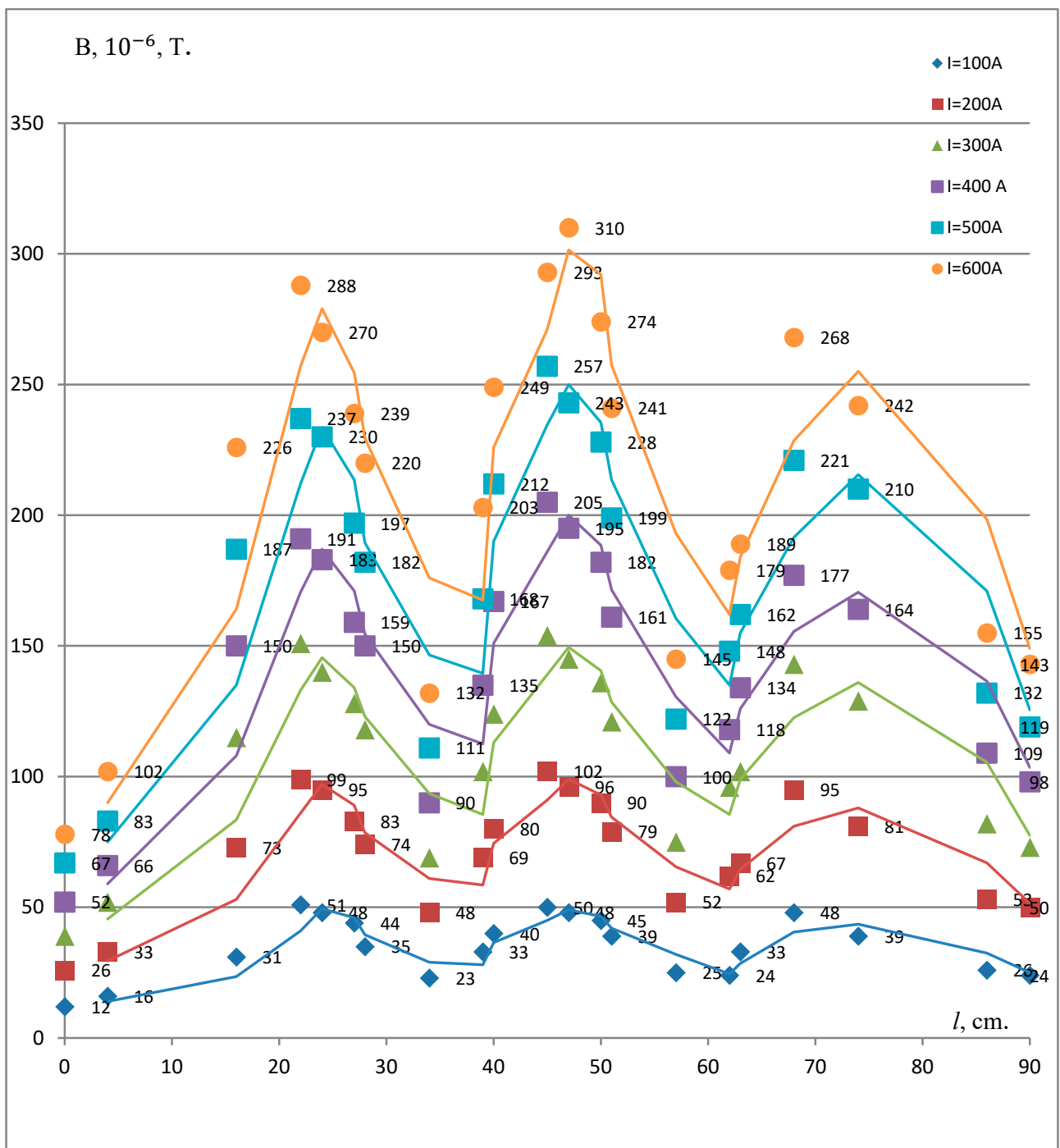
**Table 2.** Accounting coefficient  $K_{acc}$  under rated three-phase operation mode of the electrical installation of cell 1 and two-phase short circuit between phases A and C in the electrical installation of cell 2.

I, A	L, cm			
	0	22	45	68
100	12/5	51/0.57	47/0.5	48/0.5
200	26/9	99/1	96/1	95/1
300	39/12	151/1.4	145/1.6	142/1.6
400	52/16	187/1.7	195/2.2	177/2.2
500	67/19	237/1.9	243/2.8	221/2.8
600	77/22.5	288/2.05	293/3.4	268/3.42

**Table 3.** Accounting coefficient  $K_{acc}$  under rated three-phase operation of the electrical installation of cell 1 and a single-phase short circuit in phase A in the electrical installation of cell 2.

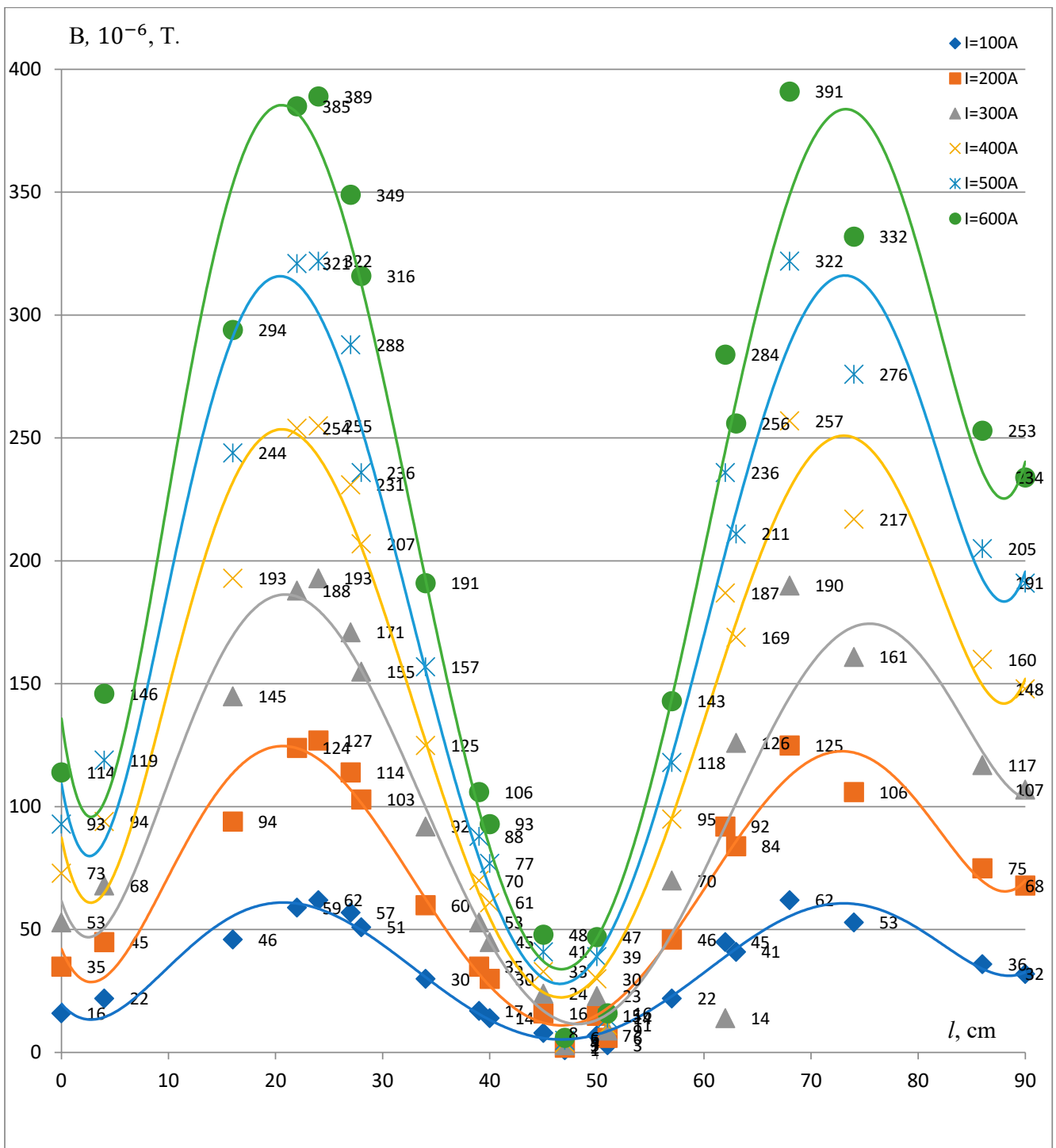
I, A	L, cm			
	0	22	45	68
100	12/10	51/3.5	47/3	48/3
200	26/22	99/8	96/7	95/6.3
300	39/35	151/12	145/11	142/9
400	52/50	187/17	195/15	177/12
500	67/60	237/22	243/19	221/16
600	77/76	288/27	293/22.3	268/19





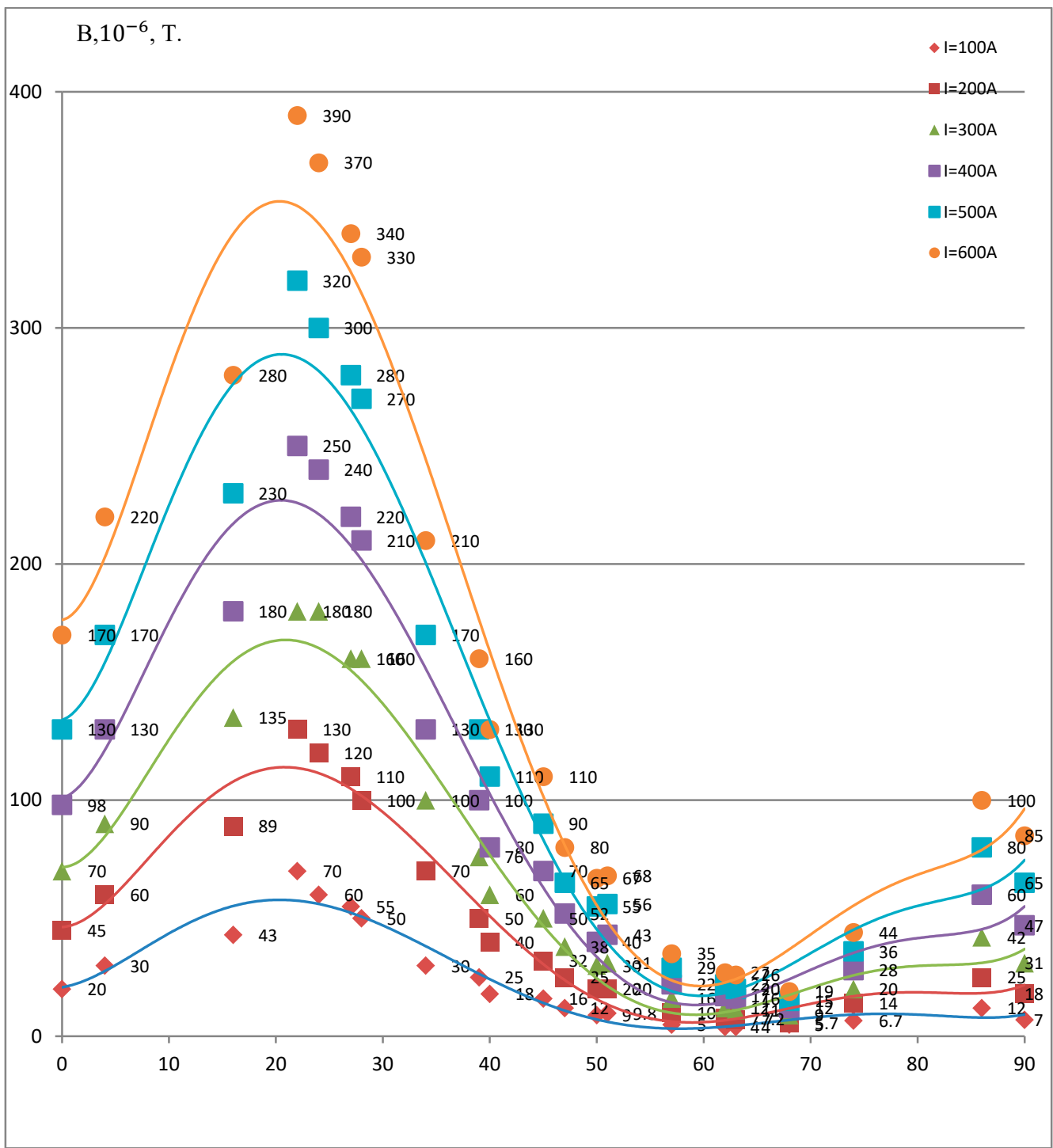
(a)

Figure 2. Cont.



(b)

Figure 2. Cont.



**Figure 2.** Dependence of magnetic induction on the current flowing through (a) three (ABC); (b) two (AC); and (c) one (A) busbars of the working cell.

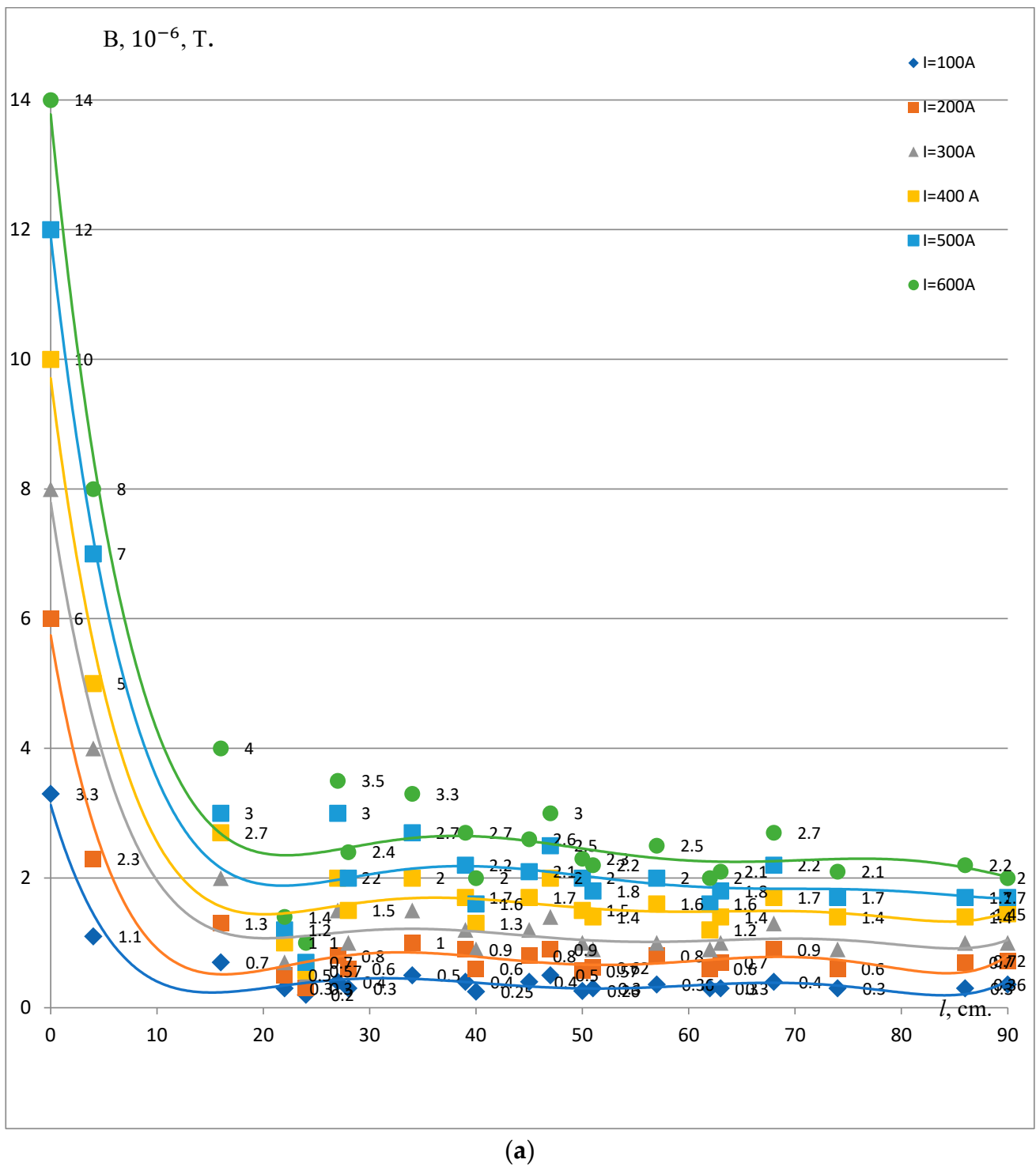
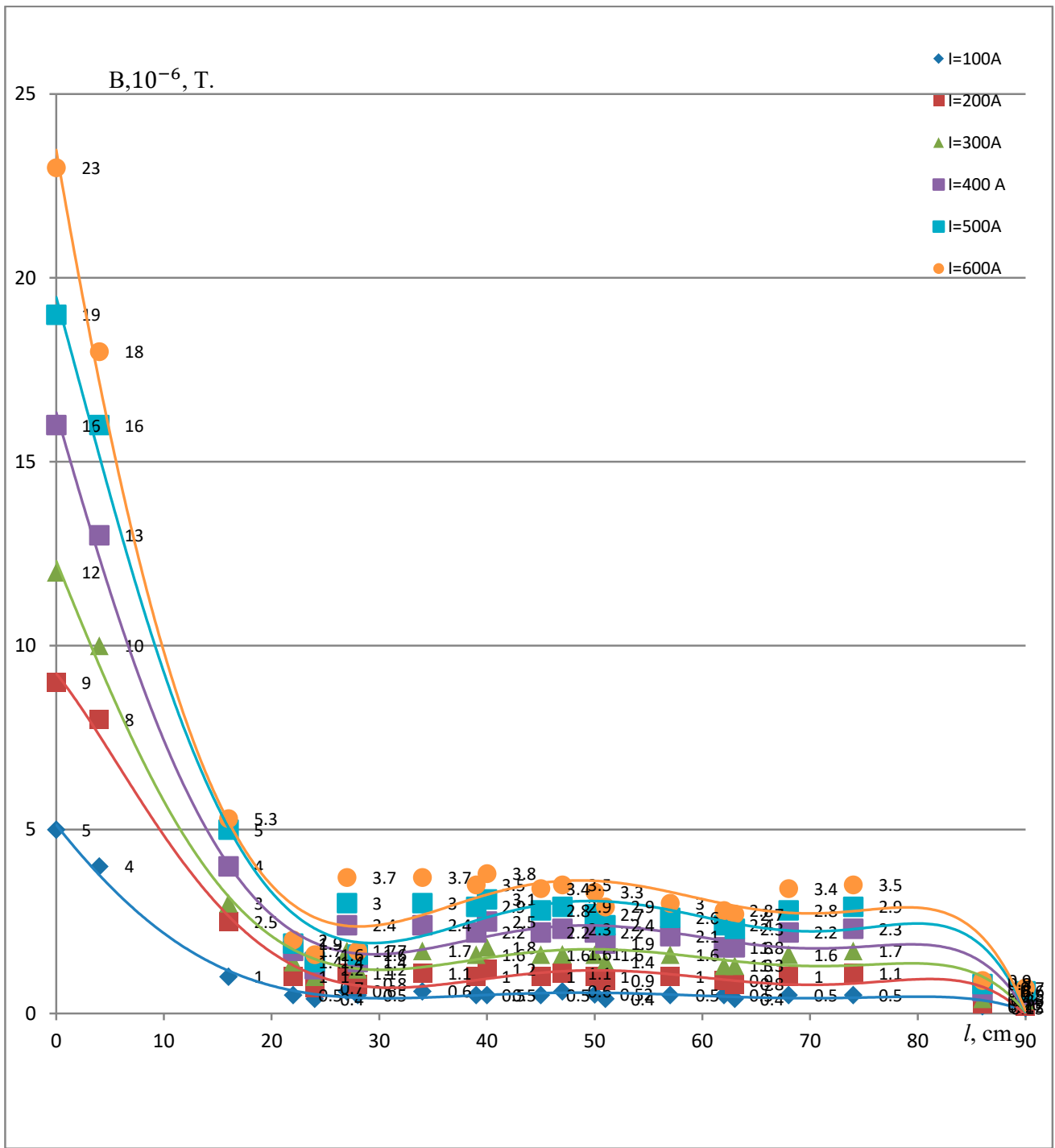


Figure 3. Cont.



(b)

Figure 3. Cont.



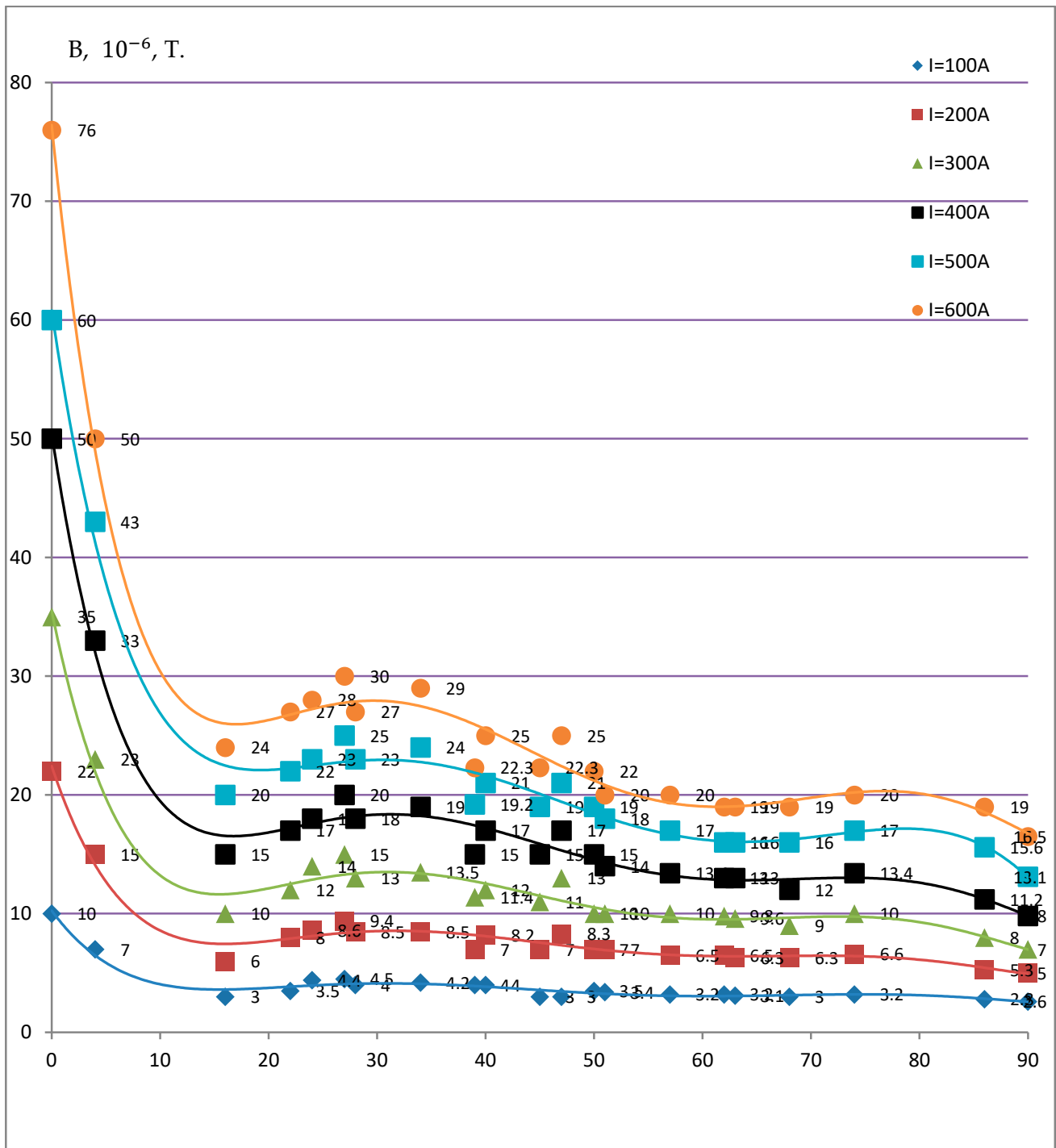


**Figure 3.** Dependence of the magnetic induction value on the current flowing through (a) three (ABC); (b) two (AC); and (c) one (A) busbars of cell 2.

**5. Overcurrent Protection with Remote Selection of Setpoint**

For the remote selection of the setpoint (operating current) of the suggested resource-saving reed switch overcurrent protection for electrical installations connected to a switchgear cell, the protection device is mounted inside the cell (Figure 4).

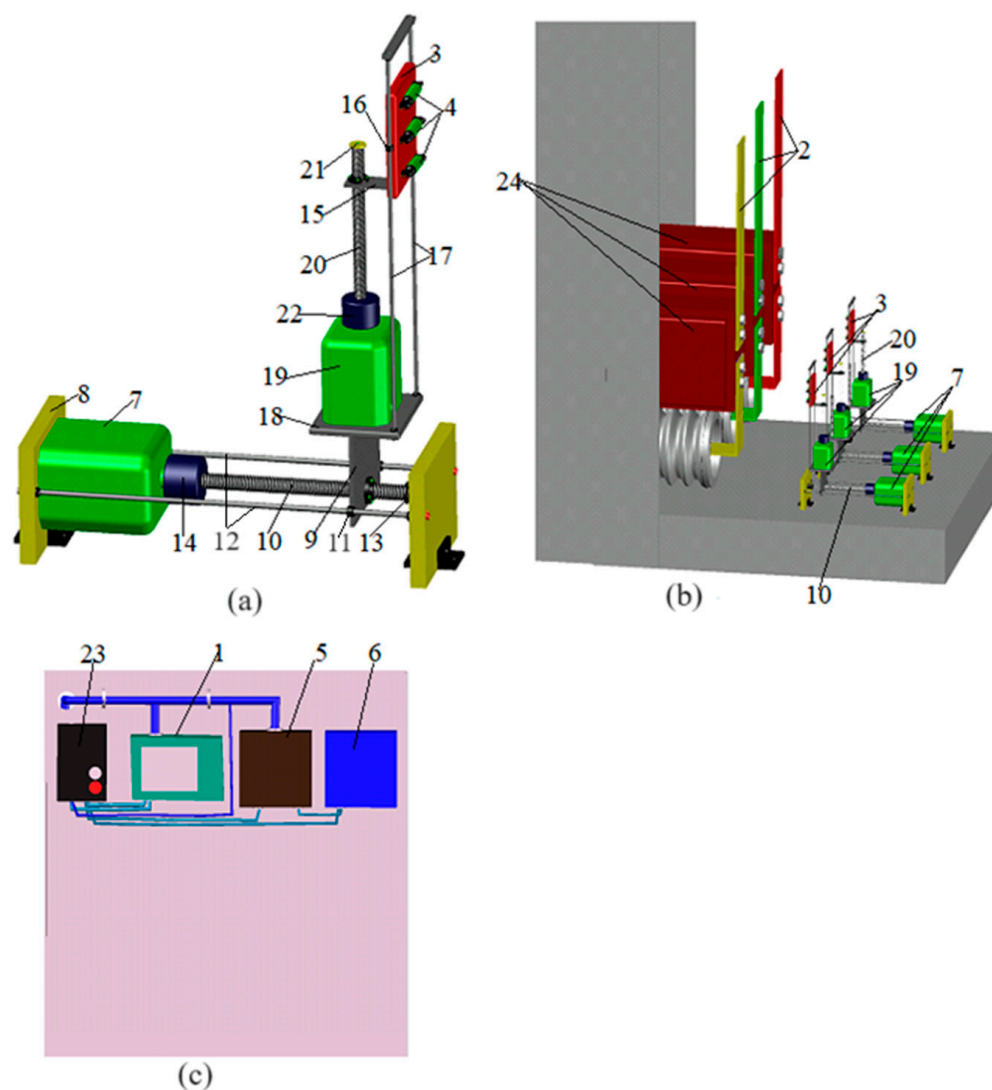


**Figure 4.** Resource-saving overcurrent protection device: (a) device components; (b) protection device mounted inside switchgear cell; (c) its control unit.

The setpoint is selected by the program of microcontroller 1, which controls the distance between current-carrying busbar 2 of each phase and plate 3 on which reed switches 4 are mounted (Figure 4a,b). One of three reed switches 4 is used for one current protection; the other two reed switches are used, for example, for current cut-offs and voltage-monitored overcurrent protection. In the bus compartment of the cell, e.g., K-63 series, three blocks of reed switches 4 are mounted at a safe distance of 12 cm [29,31], recommended by the Rules for Electrical Installations, from current-carrying busbars 2. Starting (time relay) 5 and executive (intermediate relay) 6 bodies are connected to these blocks (Figure 4c).

Transverse movement of plate 3 with reed switches 4 up to current-carrying busbar 2 is performed by switching on first microelectric motor 7. This motor is fixed to first bar 8. It moves plate 3 along first drive shaft 10 clockwise or counterclockwise in the direction “towards or from” current-carrying busbar 2 with the help of first holder 9 (Figure 4a,b). First lugs 11 are located on both sides of first holder 9, through which first traveling axes 12 pass during movement. Plate 3 moves towards busbar 2 up to hollow cylinder 13 and from busbar 2 to first coupling 14.

Plate 3 with mounted reed switch 4 and second lugs 16 is fixed on second holder 15; second traveling axes 17 pass through lugs 16 when plate 3 moves. Second bar 18 with

second microelectric motor 19 and second drive shaft 20 mounted on it is fixed on first holder 9; limit stop 21 is mounted at the end of the drive shaft (Figure 4a).

In-plane movement of plate 3 with reed switches 4 along current-carrying busbar 2 is performed by switching on microelectric motor 19 clockwise or counterclockwise. Plate 3 with reed switches 4 moves “up and down” along second drive shaft 20. Second lugs 16 are located on both sides of plate 3, through which second travel axles 17 pass during the movement (Figure 4a,b). Plate 3 moves up to limit stop 21 in the upper part and to second coupling 22 in the lower part. The overcurrent protection device is supplied from circuit breaker 23 (Figure 4c).

Before placing the overcurrent protection device in a cell, it is necessary to calculate the distance and angle at which reed switches 4 should be located with respect to magnetic field lines produced by the current in current-carrying busbars 2 before reed switches 4. The overcurrent protection operating current in busbars 2 should also be calculated. After that, reed switches 4 with the specified magnetomotive force are selected according to the factory tabulated data (Figure 4a,b). In the rated load mode of the electrical installation connected to the cell, the current flowing through current-carrying busbars 2 does not exceed the maximal operating current. Reed switches 4 are affected by a magnetic field with the induction insufficient to trigger them. As a result, the overcurrent protection fails to operate.

When a short circuit occurs at the terminals of the protected installation, the current in current-carrying busbars 2 of the cell becomes greater than the operating current of the protection. This increases the magnetomotive force acting on one of reed switches 4, which closes its contacts and sends a signal to the input of time relay 5, which, after a time delay, sends a signal to the input of actuator 6. Actuator 6 is triggered and sends a tripping signal to the circuit breaker of the electrical installation (Figure 4c). The protected electrical installation is disconnected from the general electrical network. The suggested overcurrent protection does not use measuring current transformers with metal cores 24.

An example of selecting the setpoint for the suggested overcurrent protection is described in Appendix A.

## 6. Discussion

The experiments with electrical current flowing through three current-carrying busbars (under rated operation mode of the electrical installation connected to cell 1) have shown that for the first position of plate 26 inside cell 1 and three rows of inductance coils, the electromotive force takes maximal values at certain points, 22, 47, and 68 cm for the distance  $h = 12$  cm; 22, 47, and 74 cm for the distance  $h = 18$  cm; and 16, 47, and 74 cm for  $h = 24$  cm, as well as 22, 45, and 74 cm for  $h = 18$  cm and 22, 50, and 86 cm for  $h = 24$  cm, respectively, from three second busbars 18 of cell 1. For the second and third positions of plate 26 and three rows of inductance coils, the electromotive force is maximal at the following points: 0, 23, 45, and 68 cm for the first row; 0, 24, 45, and 70 cm for the second row; and 0, 24, 47, and 64 cm for the third row. The electromotive force values are numerically lower when plate 26 is in the first position than when it is in the second and especially the third position, because the inductance coils are maximally close to the internal metal structures of cell 1, which produce additional magnetic fields (interference), in the second and third positions. The electromotive force values are minimal at the points 34 and 57 cm for all three rows of ICs of cell 1. This corresponds to almost  $\frac{1}{2}$  of the distance between the centers of the current-carrying busbars of the phases, 33.5 cm between A and B and 56.5 cm between B and C, if the distance is calculated from the left to the right side of cell 1.

When the current flows through two second busbars 18, the electromotive force values are the highest at the following points: in the case of two-phase short circuits between phases A and B, at 45 and 68 cm; between phases A and C, at 24 and 68 cm; and between phases B and C, at 22 and 47 cm.

When current flows through one second current-carrying busbar 18, the highest values of electromotive force were at the following points: in the case of a single-phase short circuit in phase A, at about 68 cm; in phase B, at 47 cm; and in phase C, at 22 cm.

## 7. Conclusions

Recommendations for creating a protection device for electrical installations connected to a switchgear cell will be as follows. The points for mounting a reed switch protection inside cell 1 are selected based on the induction maxima. According to the results of our study, measuring elements of the protection is advisable to mount at the first position of plate 26, in front of the center of the axes of second current-carrying busbars 18 at the distance  $h = 12$  cm from them. Taking into account the difficulty of protection detuning, it is not desirable to mount measuring elements of the protection (inductance coils) when plate 26 is in the second and third positions, because of the strong effect of the above-mentioned internal metal structures of cell 1, which produce additional interference. Experiments with switchgear cells showed a possibility of creating an overcurrent protection based on reed switches, which can be an alternative to traditional current protections made with the use of measuring current transformers.

Benefits of the research: Experiment studies and development on their basis overcurrent protection of various electrical installations connected to switchgear cells provide a possibility of saving significant amounts of copper, steel, and high-voltage insulation due to avoiding the use of traditional measuring current transformers with metal cores. There is also a possibility of reducing the size and weight of a switchgear cell (by approximately 30%), since it will have no compartment for measuring current transformers.

Research perspectives and field experiments: Experimental research of current protections based on inductance coils, including those for other voltage classes, will be continued in the following directions: development of resource-saving current protections for various electrical installations connected to a cell and for free-standing electrical installations; the research and creation of the differential protection of switchgear cells and connections connected to it; gas protections of power transformers without using traditional measuring transformers.

Main consumers of the research results: The results can be used by large and small industrial enterprises of various forms of ownership, the scientific community, electric power stations, and substations of plants.

## 8. Patents

(1) Issabekov Dauren Jambulovich, KZ Patent "Installation for investigation of electromagnetic field inside a complete switchgear", No 34420, Bulletin No 25, 2020, <https://gosreestr.kazpatent.kz/Invention/Details?docNumber=294569> (accessed on 11 January 2024).

(2) Issabekov Dauren Jambulovich, KZ Patent "Design for determining the parameters of the electromagnetic field inside the cell of a complete switchgear", No 35129, Bulletin No 26, 2021, <https://gosreestr.kazpatent.kz/Invention/Details?docNumber=327040> (accessed on 5 January 2024).

(3) Issabekov Dauren Jambulovich, Temirtayev Ilyas Askarovich, KZ Patent "Differential protection of power transformers", No 35665, Bulletin No 2, 2022, <https://gosreestr.kazpatent.kz/Invention/Details?docNumber=335617> (accessed on 4 March 2024).

**Author Contributions:** Conceptualization: D.D.I.; Research: D.D.I. and Z.B.M.; Writing—preparation of the initial draft: V.P.M. and D.S.U.; Writing—reviewing and editing: D.D.I. and A.P.K.; Supervision: A.P.K. and Z.B.M.; Project Administration: V.P.M. and D.S.U.; Obtaining funding: D.D.I. All authors have read and agreed to the published version of the manuscript.

**Funding:** This research was funded by the Committee on Science of the Ministry of Science and Higher Education of the Republic of Kazakhstan (Grant No. AP14972954).

**Data Availability Statement:** Original material presented in the research is included in the article.

**Conflicts of Interest:** All authors of the submitted work declare that they have no known personal relationships or competing financial interests that could influence the work presented in this research article.

### Appendix A. Selection of Overcurrent Protection Setpoint

The selection of overcurrent protection setpoints is initially considered according to the selection of setpoints for conventional current protection. But in conventional current protection, it receives information in the form of current from current measuring transformers. The conventional current protection is connected to these current transformers. The presented resource-saving protection made on reed switches is not connected to the measuring current transformers and, accordingly, does not receive power from them. The principle of the presented protection is based on the phenomenon of magnetic induction, which occurs around the conductor with current. In this case, the current conductor is the current-carrying busbars of the switchgear panel. For example, at the rated current of the electrical installation connected to the panel, there will be one value of magnetic induction around the current-carrying busbar. In the event of a short circuit in the electrical installation connected to the cell and, consequently, in the current-carrying busbars of the cell, the current value increases sharply. The magnetic induction also increases. This increased magnetic induction triggers the reed switch. Then, the circuit breaker of the cell is tripped, disconnecting the damaged electrical installation from the general electrical network. The selection of settings of the presented protection is carried out taking into account that the Biot–Savart–Laplace law is applicable for an infinitely long and thin conductor, which does not take into account the influence of interference and errors caused by the inaccuracy of reed switch installation at a given point, alternating current flow, field distortion, and the shape of the busbar. The selection of the tripping setpoint is made by entering the coefficients into the formula of the Biot–Savart–Laplace law, allowing this selection to be made when there is magnetic induction.

As is known, the operating current of a traditional overcurrent protection should be greater than the maximal operating current  $I_{\max}$  of the electrical installation connected to a switchgear cell. Taking into account the coefficients of detuning  $K_{\text{detuning}}$ , which considers the errors of instruments and protection devices and calculation uncertainties, and self-starting  $K_{\text{selfstart}}$  and return  $K_{\text{return}}$  coefficients [1],

$$I_{\text{protection operation}} \geq \frac{K_{\text{detuning}} \times K_{\text{selfstart}} \times I_{\max}}{K_{\text{return}}}, \quad (\text{A1})$$

However, since the action of the reed switches depends on the magnetic field strength of a conductor with current, we recalculate the operating current into the corresponding operating induction at the reed switch installation point according to the Biot–Savart law [33]. To ensure sensitivity, a reed switch is suggested to be mounted in the cross-sectional plane of second busbar 18 of cell 1 perpendicular to a straight line passing through the center of gravity of the reed switch and the axis of this busbar.

Taking into consideration that the Biot–Savart law is applicable to an infinitely long and thin conductor and ignoring the effect of interference and errors caused by inaccuracy of reed switch mounting at a given point, alternating current, field distortion, and the shape of second current-carrying busbar 18, the setpoint is selected through recalculating the operating current of the protection  $I_{\text{protection operation}}$  in the induction by the law of Biot–Savart under the following condition (Figure A1):

$$B_{\text{working cell protection operation}} \geq \mu_0 \frac{I_{\text{protection operation}}}{2\pi h} \cos\varphi = \mu_0 \frac{K_{\text{detuning}} \times K_{\text{selfstart}} \times I_{\max}}{2\pi h} \cos\varphi$$

at  $g_A = g_C$ ,

(A2)



Here,  $h$  is the distance from the axis of second current-carrying busbar 18 to the center of gravity of the reed switch;  $\varphi$  is the angle between the direction of current  $I$  and distance  $h$ ;  $\mu_0 = 4\pi \cdot 10^{-7}$  Gm/m is the magnetic constant; and  $g$  is the coefficient characterizing the geometric location of the reed switch relative to second current-carrying busbar 18.

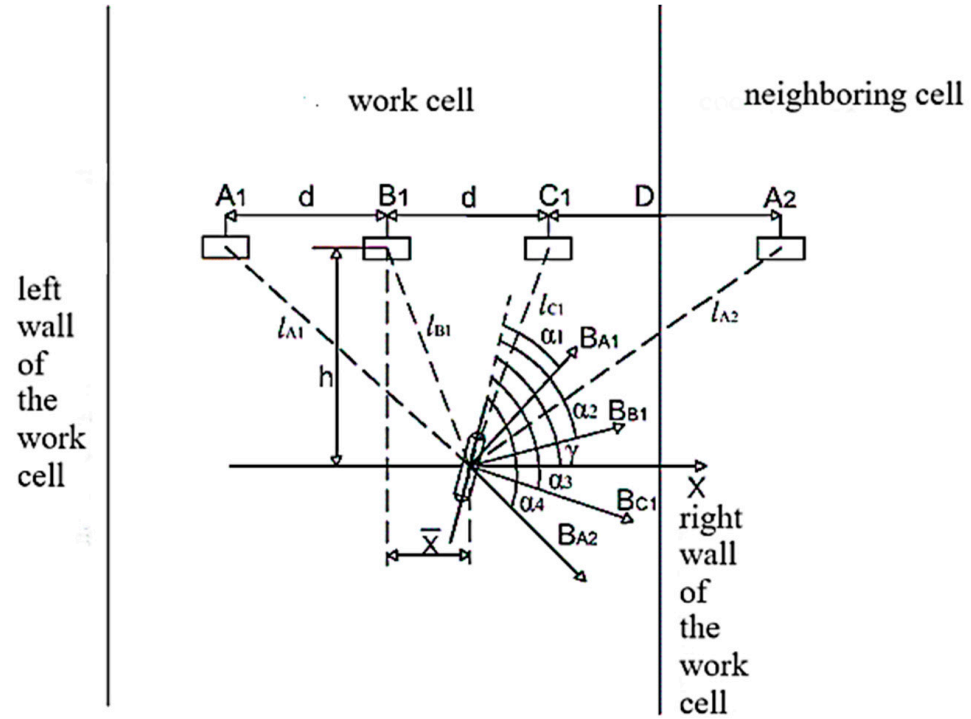


Figure A1. Position of reed switch inside working cell 1.

When designing an overcurrent protection of electrical installations connected to working cell 1 in the absence of neighboring cell 2, the induction  $B_{\text{working}}$  cubicle protection operation affecting the reed switches, located under proper phases at distances  $l_{A1}$ ,  $l_{B1}$ , and  $l_{C1}$ , is produced by the currents from the three phases, and the total magnetic field  $B_{\Sigma} = \frac{\mu_0}{2\pi}(g_A I_A + g_B I_B + g_C I_C)$  (Figure A2). In order for a reed switch to respond to the current in only one phase, for example, phase A, the influence of phases B and C is excluded by equating  $(g_B I_B + g_C I_C)$  to 0. Considering that  $I_B = -I_C$  in the case of a short circuit between phases B and C, we obtain  $g_B = g_C$ . This eliminates the influence of phase currents B and C under loads and during three-phase short circuits in the reed switch. Keeping in mind that  $I_B + I_C = -I_A$  in these modes, we obtain  $B_A = \frac{\mu_0}{2\pi}(g_A I_A - g_B I_A) = \frac{\mu_0}{2\pi} I_A (g_A - g_B)$ . The procedure for phases B and C is similar.

Due to the fact that the currents in the phases of the electrical installation of cell 1 are equal in magnitude, we assume them to be equal to the maximal operating current  $I_{\text{max}}$ . The induction of the neighboring cell  $B_{\text{neighboring}}$  cubicle occurs if there is neighboring cell 2 next to working cell 1 and if three-phase or two-phase short circuits occur in electrical installations connected to cell 2.

The presence of current on the body of cell 1 (not in current-carrying busbars 18), where a reed switch is mounted, is not taken into account due to its absence in normal operation. This is due to the fact that this current occurs in two cases: (a) in single-phase short circuits to earth; (b) in double short circuits, when, for example, one of the faults occurred in cell 1. In the first case, the short-circuit currents are small in magnitude and the induction of the magnetic field produced by them can be neglected. In the second case, if the currents in cell 1 increase the induction acting on the reed switch, this increases the sensitivity of the current protection; if they decrease the induction, this should be taken into account when determining the sensitivity.

The magnetic induction also depends on the accuracy of reed switch mounting at a given point, which should be no worse than 3%. The effect of this error on the induction  $B_{\text{working cell protection operation}}$  from the current-carrying phase opposite to which the reed switch is mounted can be neglected, which provides a margin of  $B_{\text{working cell protection operation}}$ . The effect of the error on the induction from the induction  $B_{\text{neighboring cell}}$  during a two-phase short circuit in the electrical installation of neighboring cell 2 can be neglected through the accounting factor  $K_{\text{acc}}$ .

The setpoint of the reed switch overcurrent protection mounted inside working cell 1 in the presence of neighboring cell 2 is selected by the formula

$$B_{\text{working cell protection operation}} = K_{\text{detuning}} \times (K_{\text{selfstart}} \times I_{\text{max}} \times G + g_{\text{neighboring cell}} \times I_{\text{SC max}}), \quad (\text{A3})$$

where  $G$  is the coefficient that takes into account the effect of the magnetic field produced under symmetrical operation modes of the electrical installation connected to working cell 1.

The coefficient characterizing the geometric position of the reed switch inside working cell 1 relative to the current-carrying busbar of the nearest phase A of neighboring cell 2 is defined as (see Figure A1)

$$g_{\text{neighboring cell}} = \frac{\cos \varphi}{2\pi l}, \quad (\text{A4})$$

where  $l$  is the distance from the reed switch to the nearest phase of neighboring cell 2.

The sensitivity coefficient  $K_{\text{sens}}$  for the electrical installations connected to working cell 1 in the presence of neighboring cell 2 is defined as

$$K_{\text{sens}} = \frac{B_{\text{short-circuit current}}}{B_{\text{protection operation}}} = \frac{I_{\text{short-circuit current}}(g_A - g_B)}{K_{\text{detuning}}(K_{\text{selfstart}} \times I_{\text{max}} \times G + g_{\text{interference}} \times I_{\text{SC max}})}, \quad (\text{A5})$$

where  $\Delta g = g_A - g_B$  is the coefficient dependent on the reed switch installation coordinates and the short-circuit type in the protected electrical installation.

The short-circuit current  $I_{\text{SC max}}$  in the maximal regime of the connected electrical installation of cell 1 is determined by the formula

$$I_{\text{SC max}} = K_{\text{reserve factor1}} \times I_{\text{max}} = K_{\text{reserve factor1}} \times I_{\text{SC min}}, \quad (\text{A6})$$

$$I_{\text{SC max}} = K_{\text{reserve factor1}} \times K_{\text{reserve factor2}} \times I_{\text{max}} = K_{\text{reserve factor}} \times I_{\text{SC min}}, \quad (\text{A7})$$

where  $K_{\text{reserve factor1}} = 1.1$  in Equation (A6) if working cell 1 is alone, without neighboring cell 2;  $K_{\text{reserve factor1}} = 1.1$  and  $K_{\text{reserve factor2}} = 2$  in Equation (A7) if there is neighboring cell 2 next to working cell 1;  $K_{\text{selfstart}} = 3-5$ ; and  $K_{\text{detuning}} = 1.3$ .

After transformations, the sensitivity factor for the electrical installation connected to working cell 1 is as follows:

$$K_{\text{sens}} = \frac{(g_A - g_B)}{K_{\text{detuning}} \times \left( \frac{K_{\text{selfstart}} \times K_{\text{acc}}}{K_{\text{reserve factor2}}} + K_{\text{reserve factor1}} \right)} \quad (\text{A8})$$

For a voltage-monitored overcurrent protection, the influence of induction (disturbances) from currents in the electrical installation connected to neighboring cell 2 can be ignored and the induction  $B_{\text{working cell protection operation}}$  is calculated by Equation (A2).

#### Appendix A.1. Verification of the Reed Switch Overcurrent Protection

The sensitivity coefficient of traditional overcurrent protection is defined as follows [1]:

$$K_{\text{sens}} = \frac{I_{\text{SC min}}}{I_{\text{protection operation}}} \quad (\text{A9})$$

As one knows, a reed switch is actuated by the magnetic field induction; therefore, it can be defined as

$$K_{\text{sens}} = \frac{B_{\text{SC min}}}{B_{\text{actuation}}}. \quad (\text{A10})$$

where  $B_{\text{SC min}}$  is the induction of the magnetic field, produced by the minimum short-circuit current flowing in second current-carrying busbars 18, at the point where the reed switch is mounted.

In Equation (A10),  $B_{\text{protection operation}}$  is substituted for  $B_{\text{actuation}}$ , because the actuation occurs at  $B_{\text{actuation}}$ , not at theoretically selected  $B_{\text{protection operation}}$ . Calculating  $B_{\text{protection operation}}$  and using the experimentally derived coefficients, we select a reed switch with actuation induction by the formula

$$B_{\text{actuation}} = \frac{\mu_0 \times F_{\text{actuation}}}{l_{\text{coils}}} = B_{\text{protection operation}}. \quad (\text{A11})$$

However, this equality is not always true. If  $B_{\text{actuation}} > B_{\text{protection operation}}$ , then it is necessary to check whether the overcurrent protection sensitivity meets the requirements. If the protection sensitivity is as required, i.e.,  $K_{\text{sens}} \geq 1.5$  at the end of the protected section and  $\geq 1.2$  at the end of the adjacent section, then we accept  $B_{\text{actuation}} = B_{\text{protection operation}}$ .

If the overcurrent protection does not meet the sensitivity requirements, the reed switch is mounted closer to the busbar. Due to the change in the reed switch position and, hence, in the  $h$  (it is decreased),  $B_{\text{protection operation}}$  is recalculated according to Equation (A4) with the new  $h$  values. Then, the new values of inductions  $B_{\text{protection operation}}$  and  $B_{\text{actuation}}$  are compared and the sensitivity coefficient of the protection  $K_{\text{sens}}$  is calculated. If the condition  $B_{\text{actuation}} \geq B_{\text{protection operation}}$  is fulfilled, we take the sensitivity coefficient  $K_{\text{sens}}$  with  $K_{\text{reserve factor1}} = 1.1$  and  $K_{\text{reserve factor2}} = 2$ .

If the overcurrent protection meets the sensitivity requirements, then the current protection is mounted; otherwise, the reed switch is moved closer to busbar 18 and the above procedure is repeated. If, however,  $B_{\text{actuation}} \leq B_{\text{protection operation}}$ , then it is necessary to move the reed switch farther from current-carrying busbar 18. In this case, the distance  $h$  is increased and the induction  $B_{\text{protection operation}}$  is recalculated by Equation (A2). Then,  $B_{\text{actuation}}$  and  $B_{\text{protection operation}}$  are compared. If  $B_{\text{actuation}} \geq B_{\text{protection operation}}$ , then the protection sensitivity is checked. If the sensitivity meets the requirement, the overcurrent protection is mounted; otherwise, the reed switch is moved farther from second current-carrying busbar 18. If there is neighboring cell 2 next to protected working cell 1, then the induction (interference) from the current in the former should be taken into account for a protection without voltage blocking. The induction value is calculated according to the above method.

## Appendix A.2. Calculation of the Overcurrent Protection

### Appendix A.2.1. Working Cell 1 Is Free-Standing, without Neighboring Cell 2

Let us calculate the operating induction for the voltage-monitored protection of the working cell  $B_{\text{working cell protection operation}}$  for a TM-2500/10 power transformer with Y/Y-0 winding connection and with a low voltage of 0.4 kV [34]. When selecting the protection operation current, we assume that the self-starting coefficient of electric motors  $K_{\text{selfstart}} = 5$  and the detuning coefficient  $K_{\text{detuning}} = 1.3$ :

$$I_{\text{max}} = \frac{S_{\text{nom}}}{\sqrt{3} \times U_{\text{nom}}}, \quad (\text{A12})$$

$$I_{\text{max}} = \frac{S_{\text{nom}}}{\sqrt{3} \times U_{\text{nom}}} = \frac{2.5}{1.73 \times 10} = 145\text{A}.$$

A reed switch is fixed at the distance  $h = 12$  cm from the center of the axis of second busbar 18 at point 68 cm. The operating induction is calculated as

$$B_{\text{working cell protection operation}} = \mu_0 \frac{K_{\text{detuning}} \times K_{\text{selfstart}} \times I_{\text{max}}}{2\pi h} = \mu_0 \left( \frac{1.3 \times 5 \times 145}{2 \times \pi \times 0.12} \right) = 1.2 \text{ mT.}$$

The interference is ignored for voltage-monitored protections.

Let us mount a KEM-1 reed switch (Ryazan Plant of Metal Ceramic Products) with the operating magnetomotive force  $F_{\text{actuation}} = 40 \text{ A} \times \text{windings}$  [35]. From the reference data for this reed switch, we take the coil length  $l_{\text{coils}} = 0.043 \text{ m}$ . Then,

$$B_{\text{actuation}} = \frac{\mu_0 * F_{\text{actuation}}}{l_{\text{coils}}} = \frac{\mu_0 * 40}{0.043} = 1.2 \text{ mT.}$$

According to the calculations,  $B_{\text{actuation}} = B_{\text{working cell protection operation}}$ ; that is, the selected reed switch meets the protection requirements.

Let us check the sensitivity of the overcurrent protection and calculate its sensitivity coefficient  $K_{\text{sens}}$ .

For a TM-2500/10-type power transformer and a cable line with the length  $l = 1 \text{ km}$ , the maximal operating current  $I_{\text{max}} = 145 \text{ A}$  between working cell 1 and this transformer. According to reference data [33], we take a cable ASB 3 × 70 with  $I_{\text{nom}} = 185 \text{ A}$ , the power transformer resistance  $X_{\text{tr}} = 2.6 \text{ Om}$ , and the total resistance  $X_{\Sigma} = 2.6 \text{ kOm}$ . In this case,  $I_{\text{SC min}} = 2 \text{ kA}$  [36].

Regarding the induction  $B_{\text{SC min}}$  of the magnetic field produced by this current flowing in current-carrying busbar 18 of working cell 1, the reed switch is mounted near

$$B_{\text{SC min}} = \frac{\mu_0 \times 2 \text{ kA}}{2 \times \pi \times 0.12} = 3.3 \text{ mT.}$$

Substituting  $B_{\text{actuation}}$  and  $B_{\text{SC min}}$  in Equation (A11) and taking  $K_{\text{reserve factor1}} = 1.1$ ,

$$K_{\text{sens}} = \frac{B_{\text{SC min}}}{1.1 \times B_{\text{actuation}}} = \frac{3.3}{1.32} = 2.5.$$

Since  $K_{\text{sens}} = 2.5 > 1.5$ , that is, the sensitivity requirement is satisfied, the reed switch overcurrent protection can be mounted at this point as an alternative to traditional current protections.

#### Appendix A.2.2. Working Cell 1 with Neighboring Cell 2: Two-Phase Short Circuit between Phases A and C in the Electrical Installation Connected to Cell 2

This type of short circuit is considered because  $K_{\text{acc}}$  is minimal in this case as compared to the other two two-phase short circuits.

Let us calculate  $K_{\text{sens}}$  for the overcurrent protection of working cell 1. A KEM-1 reed switch is fixed on the body of working cell 1, on its right inner side at a distance of 12 cm (Figure A2) from the plane of current-carrying busbars 18, at point 0 cm to protect the same-type TM-2500/10 power transformer [33]. We take  $K_{\text{detuning}} = 1.3$  in the case under study;  $K_{\text{reserve factor1}} = 1.1$ ;  $K_{\text{reserve factor2}} = 2$ ;  $K_{\text{selfstart}} = 5$ ; and  $K_{\text{acc}} = 77/22.5 = 3.4$ . The distance between the nearest current-carrying busbars of working cell 1 and neighboring 2 cells is  $D = 35 \text{ cm}$ ; the distance between phases A and B of working cell 1 is  $d_1 = 23 \text{ cm}$ ; the distance between phases B and C of working cell 1 is  $d_2 = 23 \text{ cm}$ ; the distance between phase C and the body of working cell 1 is  $d_3 = 22 \text{ cm}$ ; and the distance from the right wall of working cell 1 to the nearest current-carrying busbar of neighboring cell 2 is  $d_4 = 13 \text{ cm}$ .

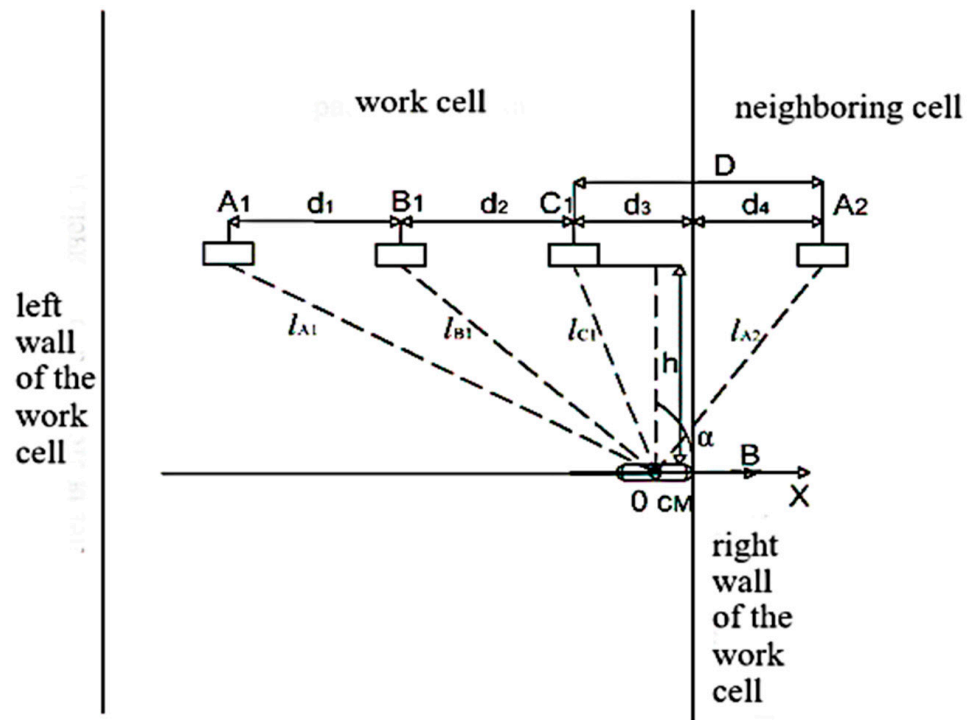


**Figure A2.** The position of the reed switch on the case of working cell 1 in the case of a two-phase short circuit between phases A and C in the electrical installation connected to neighboring cell 2.

$$g_A = \frac{\cos\alpha \times h + (d_1 + d_2 + d_3) \times \sin\alpha}{h^2 + (d_1 + d_2 + d_3)^2} = \frac{\cos\alpha \times 0.12 + 0.68 \times \sin\alpha}{0.48} = 0.25 \cos\alpha + 1.4 \sin\alpha;$$

$$g_B = \frac{\cos\alpha \times h + (d_2 + d_3) \times \sin\alpha}{h^2 + (d_2 + d_3)^2} = \frac{\cos\alpha \times 0.12 + 0.45 \times \sin\alpha}{0.22} = 0.55 \cos\alpha + 2 \sin\alpha;$$

$$g_C = \frac{\cos\alpha \times h + d_3 \times \sin\alpha}{h^2 + d_3^2} = \frac{\cos\alpha \times 0.12 + 0.22 \times \sin\alpha}{0.063} = 1.9 \cos\alpha + 3.5 \sin\alpha;$$

$$g_{\text{neighboring cell}} = \frac{\cos\alpha}{27\pi} = 0.94 \cos\alpha;$$

$$K_{\text{sens}} = \frac{(g_A - g_C)}{K_{\text{detuning}} \times \left( \frac{K_{\text{selfstart}} \times K_{\text{acc}}}{K_{\text{reserve factor2}}} + K_{\text{reserve factor1}} \right)} = \frac{-1.65 \times \cos\alpha - 2.1 \times \sin\alpha}{1.3 \times 0.94 \cos\alpha \left( \frac{3 \times 3.4}{2} + 1.1 \right)} = \left( \frac{-1.65 \times \cos\alpha - 2.1 \times \sin\alpha}{7.6 \cos\alpha} \right).$$

Let us differentiate this expression:

$$(1.65\sin\alpha - 2.1\cos\alpha) \times 7.6\cos\alpha - (-1.65\cos\alpha - 2.1\sin\alpha) \times (-7.6\sin\alpha) = 12.5\sin\alpha \times \cos\alpha - 16\cos\alpha^2 - 12.5\sin\alpha \times \cos\alpha + 16\sin\alpha^2 = 0,$$

$$-16\cos\alpha^2 = 16\sin\alpha^2,$$

$$-\text{tg}\alpha^2 = 1, \alpha = -45^\circ,$$

$$\text{Sin}\alpha = -0.707; \cos\alpha = 0.707.$$

Hence,

$$K_{\text{sens}} = \frac{-1.65 \times 0.707 - 2.1 \times 0.707}{7.6 \times 0.707} = 0.5$$



Since  $K_{sens} = 0.5 < 1.5$  (1.2), the reed switch overcurrent protection cannot be mounted at this point as an alternative to traditional current protections against two-phase short circuits.

### Appendix A.2.3. Working Cell 1 with Neighboring Cell 2: Single-Phase Short Circuit in Phase A in the Electrical Installation Connected to Cell 2

This type of short circuit is considered because it is possible to have two earth faults at two points at two different couplings, and  $K_{sens}$  is minimal as compared to the other two single-phase short circuits. A KEM-1 reed switch type is mounted in the same place as in the case of a two-phase short circuit between phases A and C (see Figure A2). For the single-phase short-circuit current  $I = 600$  A, we take  $K_{detuning} = 1.3$ ;  $K_{reserve\ factor1} = 1.1$ ;  $K_{reserve\ factor2} = 2$ ;  $K_{selfstart} = 5$  and  $K_{acc} = 77/76 \approx 1$ ;  $D = 35$  cm;  $d_1 = 23$  cm;  $d_2 = 23$  cm;  $d_3 = 22$  cm; and  $d_4 = 13$  cm.

Let us calculate  $K_{sens}$ :

$$g_A = \frac{\cos\alpha \times h + (d_1 + d_2 + d_3) \times \sin\alpha}{h^2 + (d_1 + d_2 + d_3)^2} = \frac{\cos\alpha \times 0.12 + 0.68 \times \sin\alpha}{0.48} = 0.25 \cos\alpha + 1.4 \sin\alpha;$$

$$g_B = \frac{\cos\alpha \times h + (d_2 + d_3) \times \sin\alpha}{h^2 + (d_2 + d_3)^2} = \frac{\cos\alpha \times 0.12 + 0.45 \times \sin\alpha}{0.22} = 0.55 \cos\alpha + 2 \sin\alpha;$$

$$g_C = \frac{\cos\alpha \times h + d_3 \times \sin\alpha}{h^2 + d_3^2} = \frac{\cos\alpha \times 0.12 + 0.22 \times \sin\alpha}{0.063} = 1.9 \cos\alpha + 3.5 \sin\alpha;$$

$$g_{neighboring\ cell} = \frac{\cos\alpha}{2\pi l} = 0.94 \cos\alpha;$$

$$K_{sens} = \frac{(g_A - g_C)}{K_{detuning} \times \left( \frac{K_{selfstart} \times K_{acc}}{K_{reserve\ factor2}} + K_{reserve\ factor1} \right)} = \frac{-1.65 \times \cos\alpha - 2.1 \times \sin\alpha}{1.3 \times 0.94 \cos\alpha \left( \frac{3 \times 1}{2} + 1.1 \right)} = \left( \frac{-1.65 \times \cos\alpha - 2.1 \times \sin\alpha}{3 \cos\alpha} \right).$$

Let us differentiate this expression:

$$(1.65 \sin\alpha - 2.1 \cos\alpha) \times 3 \cos\alpha - (-1.65 \cos\alpha - 2.1 \sin\alpha) \times (-3 \sin\alpha) = 5 \sin\alpha \times \cos\alpha - 6.3 \cos\alpha^2 - 5 \sin\alpha \times \cos\alpha + 6.3 \sin\alpha^2 = 0,$$

$$-6.3 \cos\alpha^2 = 6.3 \sin\alpha^2,$$

$$-\tan\alpha^2 = 1, \alpha = -45^\circ$$

$$\sin\alpha = -0.707; \cos\alpha = 0.707.$$

Then,

$$K_{sens} = \frac{-1.65 \times 0.707 - 2.1 \times 0.707}{3 \times 0.707} = 1.25$$

Since  $K_{sens} = 1.25 > 1.2$ , then the reed switch overcurrent protection can be mounted at this point as an alternative to traditional current protections against single-phase short circuits in the electrical installation connected to neighboring cell 2.

## References

1. Andreev, J.V. *Relay Protection and Automatics of Power Supply Systems*, 4th ed.; Higher School: Moscow, Russia, 2008; 608p.
2. Kazansky, V.E. *Current Transformers in Relay Protection Circuits*; Energiya: Moscow, Russia, 1969; 184p.
3. D'yakov, A. Electric-power industry in the world in early 21st century (according to the materials of the 39th CIGRE session, Paris). *Energ. Zarubezhom* **2004**, 4–5, 44–45.
4. Shneerson, E.M. *Digital Relay Protection*; Energoatomizdat: Moscow, Russia, 2007.
5. Sverdlovsk Plant of Current Transformers. Available online: <https://www.czt.ru/catalog/transformatory-toka/transformatory-toka-naruzhnoy-ustanovki/opornye1/10-kv-1/tol10iii/> (accessed on 28 February 2024).
6. Karabanov, S.M.; Maisels, R.M.; Shoffa, V.N. *Magnetically Operated Contacts (Reed Switches) and Products Based on Them*; Publishing House Intellect: Dolgoprudny, Russia, 2011.

7. Kletsel, M.Y.; Musin, V.V. About construction on reed switches of protections of high-voltage installations without current transformers. *Elektrotehnika* **1987**, *4*, 11–13.
8. Egiazaryan, G.A.; Stafeyev, V.I. *Magnetodiodes, Magnetotransistors and Their Applications*; Radio and Communication: Moscow, Russia, 1987.
9. Kotenko, G.I. Magnetoresistors. L: Energy. 1972. Available online: [https://www.studmed.ru/kotenko-gi-magnitorezistory\\_3bed601fad0.html](https://www.studmed.ru/kotenko-gi-magnitorezistory_3bed601fad0.html) (accessed on 16 February 2024).
10. Kobus, A.; Tushinsky, J. *Hall Sensors and Magnetoresistors/per. from Polish, B.I. Tikhonova, K.B. Macidonian; Khomeriki, O.K., Ed.*; Energy: Moscow, Russia, 1971.
11. Kozhovich, L.A.; Bishop, M.T. «Modern Relay Protection with Current Sensors Based on the Rogowski Coil»//*Modern Trends in the Development of Relay Protection and Automation of Power Systems: Collection of Articles. Report Int. Scientific and Technical Conf.*; Scientific and Engineering Information Agency: Moscow, Russia, 2009; pp. 39–48.
12. Kojovic', L.A.; Bishop, M. Modern protection relay with current sensors based on the Rogowski coil. Modern trends in the development of relay protection and automation of power systems. In Proceedings of the CIGRE, Moscow, Russia, 7–10 September 2009.
13. Kletsel, M.Y.; Zhantlesova, A.; Mayshev, P.; Mashrapov, B.; Issabekov, D. New filters for symmetrical current components. *Int. J. Electr. Power Energy Syst.* **2018**, *101*, 85–91. [[CrossRef](#)]
14. Kletsel, M.Y.; Musin, V.V. Selection of the operating current of the overcurrent protection without current transformers on reed switches. *Ind. Power Eng.* **1990**, *4*, 32–36.
15. Elmitwally, A.; Gouda, E.; Eladawy, S. Optimal allocation of fault current limiters for sustaining overcurrent relays coordination in a power system with distributed generation. *Alex. Eng. J.* **2015**, *54*, 1077–1089. [[CrossRef](#)]
16. Kletsel, M.Y.; Mashrapov, B.E.; Isabekov, D.D.; Amrenova, D.T. Reed-Switch-Based Relay Protection without Current Transformers. *Russ. Electr. Eng.* **2022**, *93*, 247–253. [[CrossRef](#)]
17. Issabekov, D.D. Resource-saving protections of power transformers against internal faults. *E3S Web Conf.* **2023**, *434*, 01041. [[CrossRef](#)]
18. Paladhi, S.; Pradhan, A.K. Resilient protection scheme preserving system integrity during stressed condition. *IET Gener. Transm. Distrib.* **2019**, *13*, 3188–3194. [[CrossRef](#)]
19. de Andrade Ferreira, R.S.; de Araujo, J.F.; Andrade, F.L.M.; Costa, E.G.; Guerra, F.C.F. Influence of electromagnetic forces in the gaps of a protective CT. *IET Sci. Meas. Technol.* **2018**, *12*, 872–877. [[CrossRef](#)]
20. Zhu, K.; Han, W.; Lee, W.K.; Pong, P.W.T. On-Site Non-Invasive Current Monitoring of Multi-Core Underground Power Cables With a Magnetic-Field Sensing Platform at a Substation. *IEEE Sens. J.* **2017**, *17*, 1837–1848. [[CrossRef](#)]
21. Chen, Y.; Huang, Q.; Khawaja, A.H. Interference-rejecting current measurement method with tunnel magnetoresistive magnetic sensor array. *IET Sci. Meas. Technol.* **2018**, *12*, 733–738. [[CrossRef](#)]
22. Zhou, M.; Centeno, V.; Arun, J.S.T.; Phadke, G. Calibrating Instrument Transformers with Phasor Measurements. *Electr. Power Compon. Syst.* **2012**, *40*, 1605–1620. [[CrossRef](#)]
23. Nascimento, I.M.; Brígida, A.C.S.; Baptista, J.M.; Costa, J.C.W.; Martinez, M.A.G.; Jorge, P.A.S. Novel optical current sensor for metering and protection in high power applications. *Electr. Power Compon. Syst.* **2016**, *44*, 148–162. [[CrossRef](#)]
24. Gurevich, V. *Electrical Relay. Device, Principle of Operation and Application*; SOLON-PRESS: Moscow, Russia, 2011; p. 688.
25. Isabekov, D. Device for Gas Protection of the Transformer on Magnetically Controlled Contacts. KZ Patent № 34422, 26 June 2020. Bulletin № 25. Available online: <https://gosreestr.kazpatent.kz/Invention/Details?docNumber=287805> (accessed on 15 January 2024).
26. Isabekov, D. Design for Oil Level Control in Transformer on Reed Switches. KZ Patent № 35386, 26 November 2021. Bulletin № 47. Available online: <https://gosreestr.kazpatent.kz/Invention/Details?docNumber=330085> (accessed on 26 February 2024).
27. Issabekov, D.D. Multipurpose Power System Protection Set that Provides Constant Remote Serviceability Control. In Proceedings of the 2022 International Conference on Industrial Engineering, Applications and Manufacturing (ICIEAM), Sochi, Russia, 16–20 May 2022; pp. 35–39. [[CrossRef](#)]
28. Yury, I.; Martirosyan, A. The development of the soderberg electrolyzer electromagnetic field's state monitoring system. *Sci. Rep.* **2024**, *14*, 3501. [[CrossRef](#)] [[PubMed](#)]
29. Doroshev, K.I. *Complete Switchgears 6–35 kV*; Energoizdat: Moscow, Russia, 1982; 376p.
30. Complete Distribution Device with Voltage 6–10, kV. KRUI K-63. *Technical Information*; Open Public Association Siberian Plant “Electroshield”: Novosibirsk, Russia, 2015.
31. Relay MKU 48. JSC “Irkutsk Relay Plant”. Available online: [https://irzirk.ru/catalog/element/rele\\_mku\\_48s\\_ra4500136\\_ra0450002\\_tu/](https://irzirk.ru/catalog/element/rele_mku_48s_ra4500136_ra0450002_tu/) (accessed on 10 January 2024).
32. *Order of the Minister of Energy of the Republic of Kazakhstan. Rules for the Device of Electrical Installations of the Republic of Kazakhstan: Approved by the Ministry of Energy of the Republic of Kazakhstan*; Adilet, Ministry of Justice of the Republic of Kazakhstan: Astana, Kazakhstan, 2015. Available online: <https://adilet.zan.kz/rus/docs/V1500010851> (accessed on 10 January 2024).
33. Bessonov, L.A. Theoretical bases of electrical engineering. In *Electromagnetic Field*, 9th ed.; Gardariki: Moscow, Russia, 2001; 317p.
34. Neklepaev, B.N.; Kryuchkov, I.P. *Electrical Part of Power Stations and Substations: Reference Materials for Course and Diploma Design: A Textbook for Universities-4 Izdu, Rev*; Energoatomizdat: Moscow, Russia, 1989; 608p, Available online: <https://ofaze.ru/wp-content/uploads/2019/12/neklepaeva-spravochnik.pdf> (accessed on 1 February 2024).

35. Joint Stock Company “Ryazan Plant of Metalloceramic Devices”. Available online: <http://www.rmci.ru/reeds/product/id/19> (accessed on 7 February 2024).
36. Shabad, M.A. *Calculations of Relay Protection and Distribution Automation Networks*, 3rd ed.; Energoarotizdat. Lenin r. Department: Leningrad, Russia, 1985; 296p, Available online: <https://www.elec.ru/library/nauchnaya-i-tehnicheskaya-literatura/raschety-rza-raspr-setej/> (accessed on 12 March 2024).

**Disclaimer/Publisher’s Note:** The statements, opinions and data contained in all publications are solely those of the individual author(s) and contributor(s) and not of MDPI and/or the editor(s). MDPI and/or the editor(s) disclaim responsibility for any injury to people or property resulting from any ideas, methods, instructions or products referred to in the content.